Green synthesis of robust superhydrophobic antibacterial and UV blocking cotton fabrics by dual stage silanization approach

Neha Agrawal,[a] Jasmine Si Jia Tan,[a] Pearlie Sijia Low,[a] Eileen Wen Mei Fong,[a] Yuekun Lai,[b,c] Zhong Chen[a]*

[a] School of Materials Science and Engineering, Nanyang Technological University, 50 Nanyang Avenue, Singapore 639798, Singapore.

[b] College of Chemical Engineering, Fuzhou University, Fuzhou 350116, PR China.

[c] College of Textile and Clothing Engineering, Soochow University, Suzhou 215123, PR China.

*Corresponding Authors E-mail: ASZChen@ntu.edu.sg

Abstract

Synthesis of multi-functional fabrics with long-lasting durability remains a quest for researchers in the past decade. In this work, robust coatings on cotton fabrics for superhydrophobic, antibacterial, and UV blocking functionalities by a dual stage silanization technique has been reported. Aminopropyltriethoxysilane (APTES) is utilized as a silane cross-linker to anchor zinc oxide (ZnO) nanoparticles to the pristine cotton fabric surface, followed by modification with a silane hydrophobe, hexadecyltrimethoxysilane (HDTMS). This dual silanization approach results in highly functional fabrics displaying superhydrophobicity with a water contact angle of 154°, water shedding angle of 2°, antibacterial activity up to 98% and UV blocking ability more than 200 times of pristine cotton. The as-prepared fabrics displayed excellent durability against abrasion, ultrasonic washing, immersion in different pH solutions, and UV irradiation. Moreover, the air permeability and flexural rigidity of the fabric were still within the required breathability

and wearer comfortability for clothing applications. The reported process is simple, cost-effective and green, showing great promise for large scale production of multi-functional fabrics.

Keywords: superhydrophobic, antibacterial, UV blocking, ZnO nanoparticles, multi-functional fabrics

1. Introduction

A water droplet fallen on a lotus leaf surface rolls away easily, carrying the dirt particles along with it. This self-cleaning phenomenon, famously called as the 'lotus effect' was first studied by Barthlott and Ehler in 1997.[1] The presence of dual micro-/nanoscale roughness combined with low surface energy on the leaf surface results in high water contact angle (WCA) > 150° and low sliding angle (SA) < 10°.[2] Such a surface termed as 'superhydrophobic' or 'ultrahydrophobic', has now found myriad applications in our day-to-day lives. Superhydrophobic coatings are now being extensively investigated for applications in automobile, aerospace, building, marine, and clean energy industries. They are also explored on flexible substrates such as non-woven materials like paper for bandages,[3] and woven materials like textiles for clothing, oil-water separation, food-packaging and healthcare applications.[4]

Surface modification of the textiles has gained increasing attention due to the flexibility, easy availability and inexpensiveness of the raw materials. Superhydrophobicity improves the performance of the fabric, enhances the shelf life by reducing the number of laundering cycles, and aids in minimizing the expenditure of energy and resources in maintaining these materials. Various researchers have successfully demonstrated the synthesis of superhydrophobic fabrics,[5]

and additional functions like antibacterial activity,[6] UV blocking,[7] electrical conductivity,[8] flame redardancy,[9] photocatalytic activity,[10] and self-healing ability,[11] are now gaining attention.

With growing awareness among the consumers, products that are safe, eco-friendly, and in the meantime ensuring a comfortable and healthy life are in great demand nowadays. As textiles are universally utilized for manufacturing clothes and garments, synthesis of multi-functional fabrics with superhydrophobicity, antibacterial activity and UV blocking ability would result in manifold improvement of clothing performance. Incorporation of superhydrophobicity will make fabrics stain-resistant, self-cleaning and reduce laundering care.[12] Antibacterial activity over the surface will ensure resistance from foul odour and growth of contagious microorganisms under imperfect weather conditions.[13] Additionally, UV-blocking property would protect the wearer from harmful UV rays making these fabrics useful for outdoor purposes.[14] These properties would further enhance its application in healthcare, military and various other industries.

One of the most popular techniques to finish fabric surfaces with multiple functions involves the incorporation of metal/metal-oxide nanoparticles like silver,[15] copper,[6b, 16] titanium dioxide,[17] and zinc oxide.[18] Among them, zinc oxide (ZnO) nanoparticles offer antibacterial activity against a large number of bacterial species.[19] They possess high optical absorption in the ultraviolet region that not only enhances its antibacterial activity but also provides UV blocking properties.[20] Although some nanoparticles are considered to be potentially hazardous for human health, there have been no reports of carcinogenicity, genotoxicity or reproduction toxicity using ZnO nanoparticles.[20] Zn is one of the important trace elements required in the human body in the

absence of which many enzymes become inactive.[20] It is essential for cell growth,[21] and forms an important component for bones, teeth, enzymes and various proteins.[20] When compared to titanium dioxide (TiO_2), ZnO nanoparticles are far more biocompatible and non-toxic to human cells.[19] They are cost-effective when compared to noble metals like silver and gold.[22] Most importantly, ZnO nanoparticles are white in appearance, and most of the fabrics are in white colour unlike other semiconductor nanoparticles such as CuO.[23] Therefore, considering the overall advantages offered by ZnO nanoparticles, they were utilised in this work for the synthesis of multi-functional fabrics.

Various studies have been conducted to synthesize multi-functional textiles utilizing ZnO nanoparticles. However, for functionalized-fabrics to be commercially viable, durability of the coatings is of prime importance. As an example, antimicrobial and ultraviolet blocking cotton textiles were fabricated by the in-situ synthesis of ZnO nanostructures.[24] However, after 5 washing cycles, most of the nanoparticles were removed from the fabric surface, resulting in poor durability of the coating.[24] Release of nanoparticles from the surface not only diminishes coating performance, but also poses a health risk due to ingestion, inhalation, or skin contact.[25] While some have reported the loss of property after few washes,[24, 26] most have not reported any durability measurement in their work,[27] limiting its practical application. For example, in a recent work, hydrophobic antibacterial cotton fabrics were synthesized by deposition of ZnO nanoparticles prepared via hydrothermal approach. Although the fabric displayed high antibacterial performance and hydrophobicity with WCA of 124.35°, no durability studies were reported.[27a] Therefore, for research to be useful for practical applications, it is essential to conduct wash-fastness, mechanical and chemical durability tests to investigate the robustness of the

coating. Furthermore, for multi-functional fabrics to be display long-lasting durability, it is essential to establish additional chemical bonds that can anchor the nanoparticles firmly to the fabric surface.

The paper reports a novel and simple method to prepare robust coatings on cotton fabrics with superhydrophobic, antibacterial and UV blocking functionalities. To achieve this aim, a dual silanization approach was adopted where one silane coupling agent serves as a silane cross-linker to bind the ZnO nanoparticles to the fabric and the other functions as a silane hydrophobe for lowering the surface energy. The superhydrophobicity, antibacterial activity and UV blocking ability of the as-prepared fabrics were evaluated. The durability of the fabrics to mechanical abrasion, ultrasonic washing, harsh chemical solutions and prolonged UV irradiation was also determined. Lastly, the air permeability, flexural rigidity and self-cleaning performance of the fabric were assessed. This facile synthesis strategy overcomes the shortcomings of the previous works and displays tremendous potential for industrial fabrication of textiles materials with multiple functionalities.

2. Experimental Work

2.1 Materials

Cotton fabric with an individual fibre diameter of ~15 μm was obtained from Matex International Limited, Singapore. Aminopropyltriethoxysilane (APTES), Hexadecyltrimethoxysilane (HDTMS), Methanol (analytical reagent grade), ZnO nanopowder (< 50 nm in diameter) and non-

ionic detergent Triton X-100 were purchased from Sigma Aldrich and used without further purification. *Escherichia coli* (*E. coli*, ATCC® 25922™) and *Staphylococcus aureus* (*S. aureus*, ATCC® 25923™) were purchased from the ATCC distribution partner Thermo Fisher Scientific, Singapore. The cotton fabric was ultrasonically cleaned with ethanol and deionized water to remove possible contaminants and dried before further processing.

2.2 Experimental Procedure

The fabrication of multi-functional HDTMS-ZnO-APTES-Cotton fabrics follows a simple two-step process as shown in Figure 1. In the first step, ZnO nanoparticles were deposited on the cotton fabric with the aid of APTES silane cross-linker. To achieve this, APTES was pre-hydrolysed in methanol (1 vol. %) where ZnO nanoparticles were ultrasonically dispersed. For a piece of 2.5 cm × 2.5 cm cotton fabric, 12.5 mg of ZnO particles was used, which leads to a 20 g/m^2 nominal particle loading. The cotton fabric was immersed in the ZnO-APTES solution and magnetically stirred to achieve ZnO-APTES-Cotton fabric. Thereafter, the fabric was heat treated at 100 °C and washed with methanol to remove unbound silane molecules. In the second step, HDTMS was coated over the ZnO-APTES-Cotton fabric. HDTMS was pre-hydrolyzed in methanol (1 vol. %) and ZnO-APTES-Cotton fabric was immersed in the solution under magnetic stirring to allow the attachment of HDTMS over the nanoparticles and fabric surface. Subsequently, the fabric was heat treated at 100 °C and washed to obtain HDTMS-ZnO-APTES-Cotton fabric.

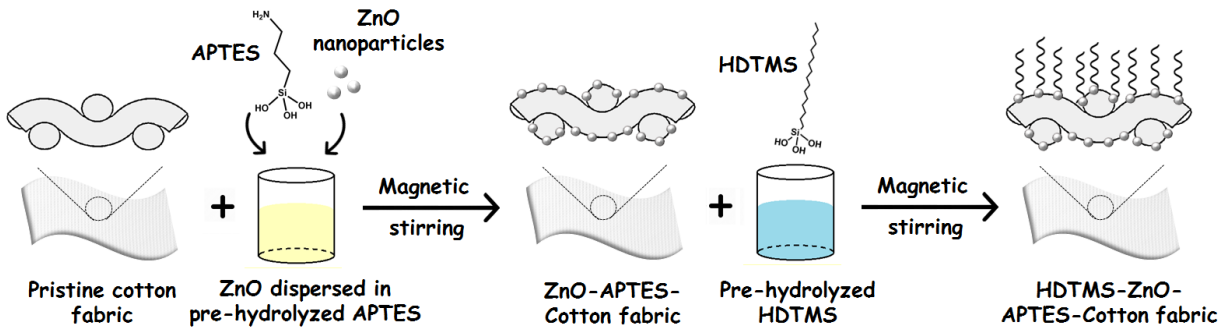

Figure 1. Schematic illustration of the two-step process for synthesis of HDTMS-ZnO-APTES-Cotton fabric

2.3 Characterization

The contact angle of the as-prepared fabrics was measured with a contact angle goniometer (OCA 20 Dataphysics, Germany). WCA and water shedding angle (WSA)[28] was recorded by placing 5 µL and 13 µL DI water droplets respectively at five equidistant positions on the fabric. The surface morphology of the fabrics and EDS spectra was obtained with a field emission scanning electron microscope (FESEM, JEOL JSM-6340F) at an acceleration voltage of 5 kV under secondary electron imaging mode. The chemical information of the as-prepared fabrics was evaluated by Fourier transform infrared spectroscopy-attenuated total reflectance (FTIR-ATR, Perkin Elmer Frontier) from 4000 cm^{-1} to 600 cm^{-1} with a resolution of 4 cm^{-1} with 32 scans per sample. The crystal structure of ZnO nanoparticles was identified by X-Ray Diffraction (XRD, Thin Film Shimadzu XRD-6000) using Cu-Kα radiation. The instrument was operated at 40 kV and 30 mA with step size of 0.02°/sec in 2θ scan mode with a glancing angle of 5°. The UV blocking ability of the as-prepared fabrics was measured following the AATCC 183-2004 Test Method[29] using a UV/Vis Spectrophotometer (Lambda 950, Perkin Elmer) in the spectral range of 400 – 280 nm at

an interval of 2 nm. The air permeability was measured using a digital air permeability tester (YG461E-11) by applying a pressure of 400 Pa on 20 cm^2 of fabric surface. The flexural rigidity was tested using a fully automated fabric rigidity tester (YGB022D), at a fixed bending angle of 41.5˚ Three samples of each coating were measured, and an average value was reported for all the characterization tests.

2.4 Antibacterial assessment

The antibacterial efficiency of the as-prepared fabrics was assessed following the AATCC 100-2004 quantitative assessment technique[30] using gram-negative and gram-positive bacteria *E. coli* (ATCC® 25922™) and *S. aureus* (ATCC® 25923™) respectively. The treated and untreated fabric samples were cut into circular swatches of 4.8 ± 0.1 cm in diameter. Luria Broth (LB) media autoclaved at 121 °C for 20 minutes was used to culture the microorganisms. The bacterial cells were tested for optical density, centrifuged and re-suspended in Phosphate Buffer Saline (PBS) solution. The fabric swatches were then inoculated with 10^5 colony forming units (CFU)/ml of bacteria and incubated at 37 °C for 24 hours. After the stipulated time, serial dilution was conducted for the estimated bacterial cells inoculated. 100 µL of the inoculum was spread evenly on the surface of the LB agar plates on a petridish and incubated at 37 °C overnight to observe the colonies. The percentage reduction of the bacterial cells was calculated by:

$$\% R = \frac{A-B}{A} \times 100 \qquad \text{Equation (1)}$$

where R is the reduction in bacterial count, A and B are the number of colonies observed for the untreated and treated fabrics respectively. Three parallel runs of each test fabric were conducted, and an average value was reported.

2.5 Durability measurements

The abrasion resistance of the as-prepared fabrics was evaluated by moving the fabrics normal to the direction of applied pressure of 4 kPa on the abradant surface of pristine cotton fabric at a speed of 3 cm/s for a distance of 11 cm per cycle. A total of 800 cycles were conducted. The wash-fastness was measured by washing the as-prepared fabrics in an ultrasound bath (275 W) at 40 ± 2 °C in a solution of Triton-X, a non-ionic detergent (1g/L) for 15 minutes. After the stipulated time, the fabrics were washed with DI water and dried. The ultrasonic washing tests were conducted for a total of 120 minutes. The chemical stability of the as-prepared fabrics was determined by subjecting them to aqueous solutions of HCl and NaOH with pH ranging from 1 to 13 for a period of 24 hours. The durability against UV radiation was determined by exposing the as-prepared fabrics to a UV lamp of 365 nm in wavelength and intensity of 72.6 mW/cm^2 for a period of 12 hours. The WCA and WSA of the fabrics were measured after these durability tests.

3. Results and Discussion

3.1 Surface morphology and contact angle analysis

A pristine cotton fabric has a completely smooth morphology (Figure 2a). After coating with 20 g/m^2 loading of ZnO nanoparticles (rod-like, < 50 nm, Figure 2b) over the pristine cotton fabric, the nanoparticles were uniformly distributed, completely covering the fabric surface area with no visible agglomeration (Figure 2c, 2d). The optimization of the ZnO nanoparticles on the fabric

surface has been discussed in detail in Section S1 of the Supporting Information. The amount of loading of the combined (ZnO + APTES) coating and the HDTMS coating was also discussed in Section S1 of the Supporting Information. The chemical composition of the HDTMS-ZnO-APTES-Cotton fabrics by the EDS spectra (Figure 2e, 2f) found that four main elements, C, O, Si, and Zn, were evenly distributed over the fabric surface. Gold was detected due to sputter coating for conducting surface for the SEM observation, along with a small percentage of aluminium impurity.

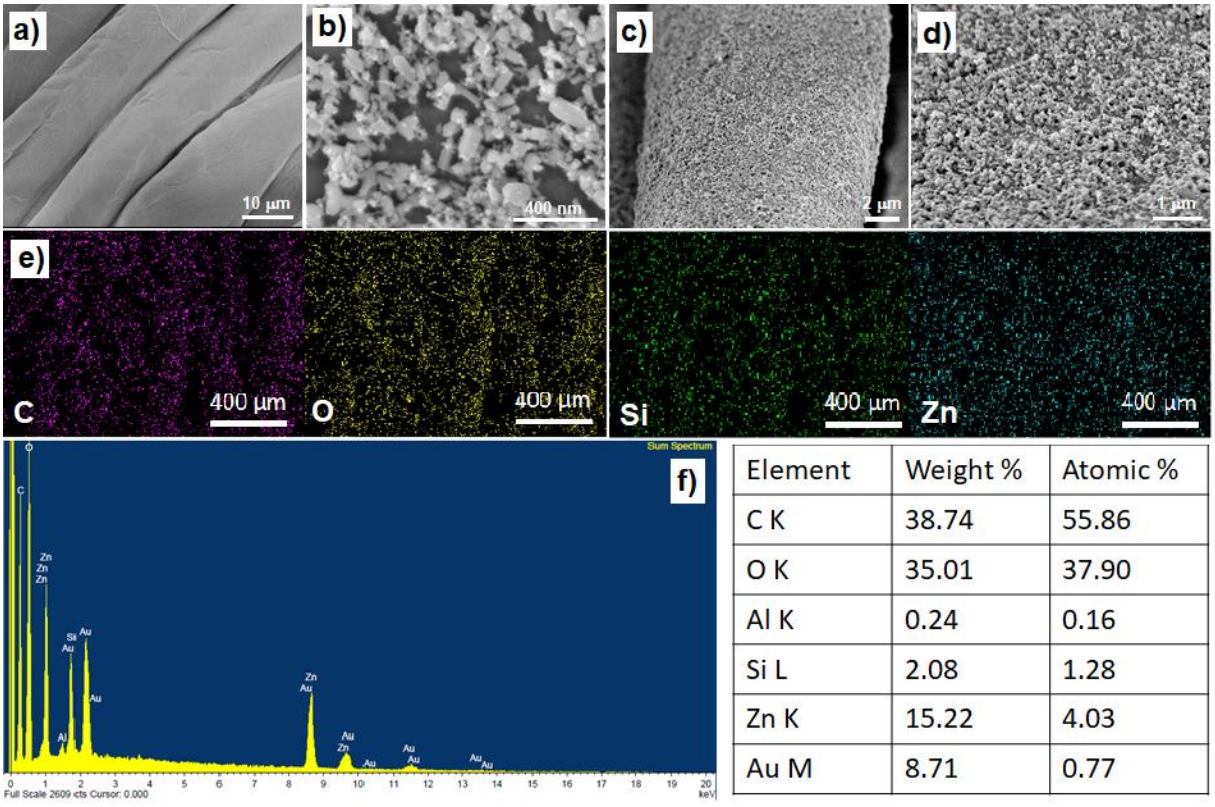

Element	Weight %	Atomic %
C K	38.74	55.86
O K	35.01	37.90
Al K	0.24	0.16
Si L	2.08	1.28
Zn K	15.22	4.03
Au M	8.71	0.77

Figure 2. FE-SEM images of a) pristine cotton fabric, b) ZnO nanoparticles, c) HDTMS-ZnO-APTES-Cotton fabric, d) higher magnification of HDTMS-ZnO-APTES-Cotton fabric; e) Element mapping of C, O, Si, Zn; f) EDS spectrum

Contact angle analysis was conducted to determine the surface wetting properties of the fabric before and after the coating. A pristine cotton fabric consists of hydroxyl groups on its surface

owing to the cellulose structure, and therefore, absorbs water displaying surface hydrophilicity (Figure 3a). Upon incorporation of the ZnO nanoparticles treated with hydrophobic APTES, the fabric displaying an average WCA of 145.8 ± 3.2° (Figure 3b). However, this surface was unstable, the water droplet was soon absorbed into the fabric probably due to exposed pristine cotton fibre surface. After coating with HDTMS, a stable superhydrophobic surface was obtained displaying a WCA of 153.5 ± 1.1° and WSA of 2.4 ± 1.2° (Figure 3c). The superhydrophobicity of the fabric is displayed in Figure 4 where spherical water droplets (tainted with dyes) are beaded over the fabric surface in comparison to pristine cotton fabric where the water droplets were absorbed quickly.

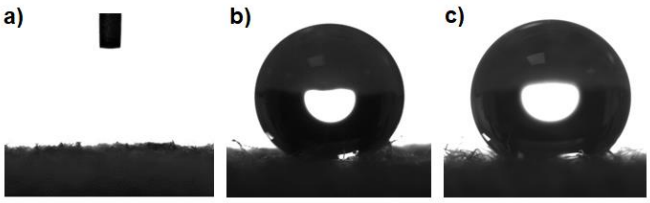

Figure 3. Goniometer images of a) pristine cotton fabric, b) ZnO-APTES-Cotton fabric, c) HDTMS-ZnO-APTES-Cotton fabric

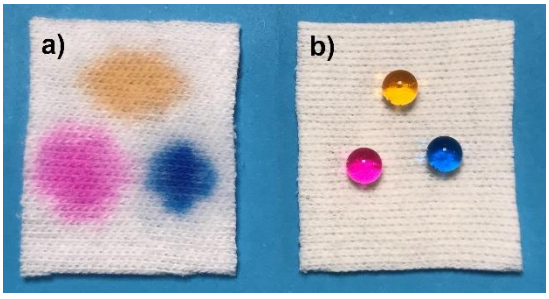

Figure 4 Photograph of dyed water droplets on a) pristine cotton fabric b) HDTMS-ZnO-APTES-Cotton fabric

3.2 Antibacterial activity assessment

The antibacterial activity of the as-prepared fabrics was evaluated by the AATCC 100-2004 quantitative assessment technique.[30] The *E. coli* and *S. aureus* colonies observed on the agar plates were counted after 24 hours of incubation and the percentage reduction was calculated as displayed in Table 1. Bacterial growth was observed for the pristine cotton fabric which was used as control, thereby resulting in no antibacterial activity. Upon deposition of ZnO nanoparticles using APTES, the fabrics displayed high reduction in the bacterial growth for both *E. coli* and *S. aureus* with up to 98% efficiency. On further coating the fabric with HDTMS, no significant reduction in antibacterial efficiency was observed. After ultrasonic washing for 2 hours, the performance declined by a small percentage, however, 96% antibacterial efficiency was maintained. These results confirm the excellent performance and durability of the as-prepared fabrics through the dual silanization synthesis approach. The growth of the *E. coli* and *S. aureus* colonies on the agar plates is shown in Figure 5 and Figure S3, respectively.

Table 1 Percentage reduction in the bacterial growth for the HDTMS-ZnO-APTES-Cotton fabrics

	Antibacterial Efficiency (%)	
Sample Name	**Escherichia coli**	**Staphylococcus aureus**
ZnO-APTES-Cotton fabric	98.2	97.8
HDTMS-ZnO-APTES-Cotton fabric	98.4	96.7
HDTMS-ZnO-APTES-Cotton fabric (washed)	97.8	96.1

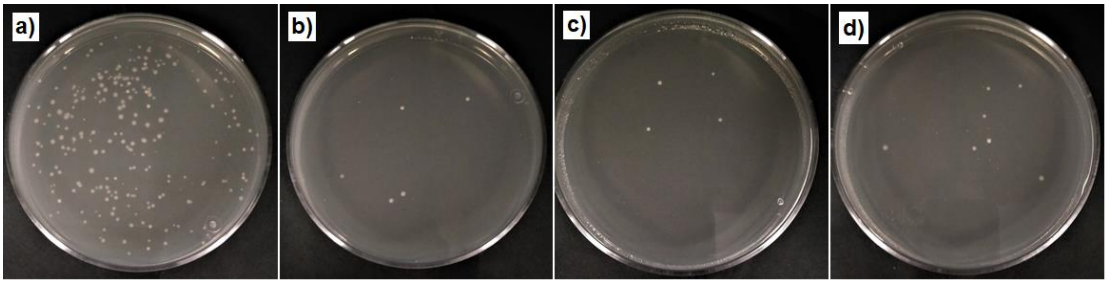

Figure 5. Growth of *E. coli* colonies on a) pristine cotton fabric b) ZnO-APTES-Cotton fabric c) HDTMS-ZnO-APTES-Cotton fabric d) HDTMS-ZnO-APTES-Cotton fabric (washed)

3.3 Coating mechanism analysis

ZnO nanoparticles consist of hydroxyl groups on its surface after water adsorption. Upon dispersion in APTES, these hydroxyl groups can either react with the silanol groups of the pre-hydrolyzed APTES or engage in hydrogen bonding with the amino group on the silane chain.[31] When brought in contact with the pristine cotton fabric, the APTES-functionalized nanoparticles are anchored to its surface by either the free silanol or amino groups of APTES. The different bond formation possible between the nanoparticles, APTES and the cellulose structure of the cotton fabric is displayed in Figure 6.

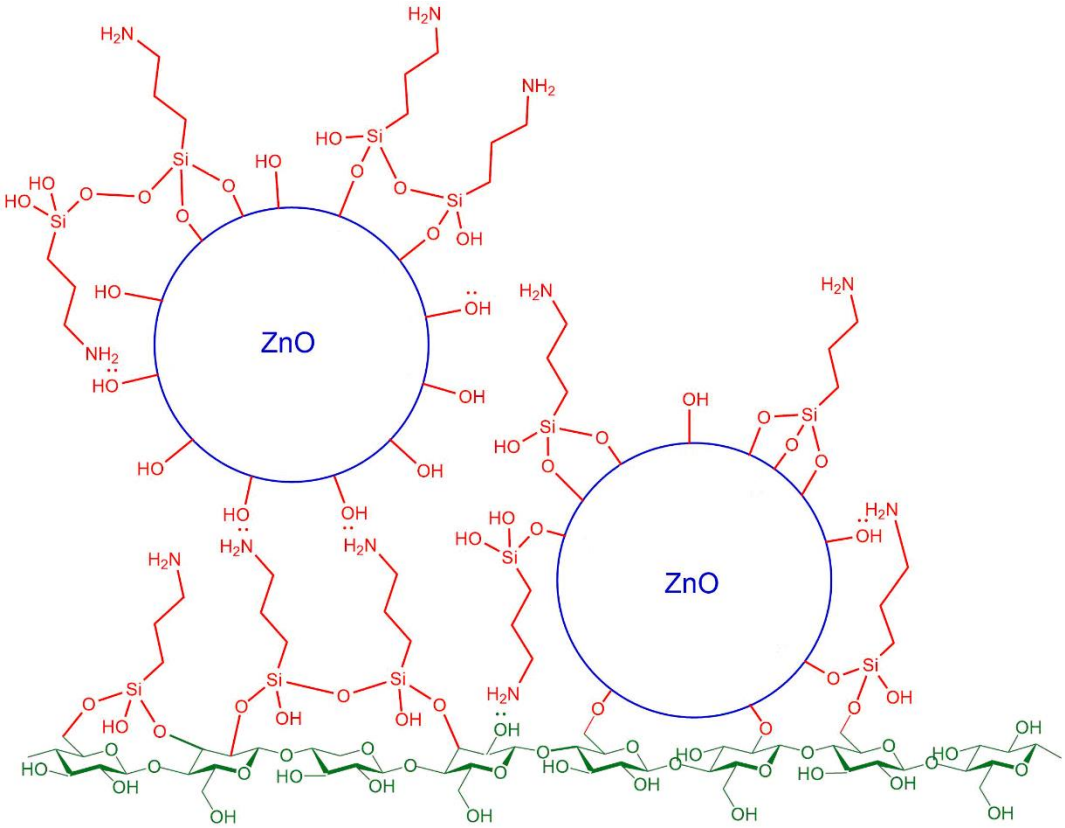

Figure 6 Proposed mechanism for attachment of APTES-functionalized ZnO nanoparticles to pristine cotton fabric

Upon further modification with HDTMS, the silanol groups of HDTMS form bonds with the free hydroxyl groups present on cellulose structure, ZnO or APTES completing the coating process. The possible bond formation between HDTMS and ZnO-APTES-Cotton fabric is illustrated in Figure 7. It is noted that Figure 6 and Figure 7 are mere representations of the type of bond formation taking place; in an actual scenario, multiple layers can be formed based on the proposed mechanism.

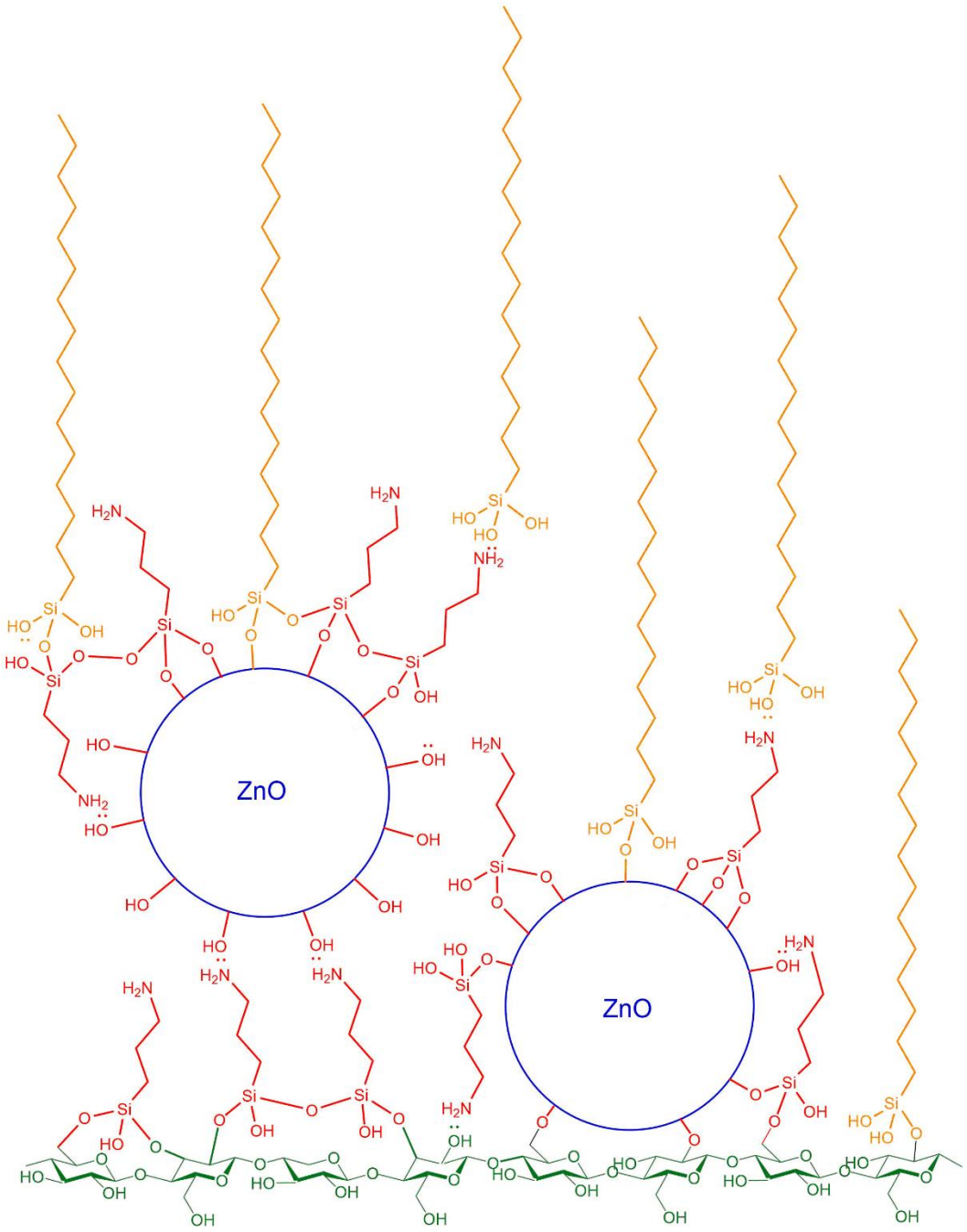

Figure 7. Proposed mechanism for the attachment of HDTMS to ZnO-APTES-Cotton fabric

To verify the proposed mechanism, FTIR results are shown in Figure 8. Before the coating, the pristine cotton fabric displays several strong peaks. The broad peak between 3600-3000 cm^{-1} is due to the hydroxyl (–OH) groups of the cellulose structure.[32] Other characteristic peaks at 2897,

1636, 1428 and 1315 cm^{-1} correspond to asymmetric stretching of $–CH_2$, –OH group from adsorbed water, and deformation vibration of C-H groups, respectively.[32] After deposition of ZnO nanoparticles using APTES, the decrease in the intensity of the broad peak between 3600-3000 cm^{-1} indicates the consumption of –OH groups on the cellulose surface for bonding. Additionally, a characteristic peak was obtained at 1561 cm^{-1} which corresponds to the deformation of NH_2 groups due to hydrogen bonding,[33] thereby confirming the role of APTES in ZnO attachment. After deposition of HDTMS, a new peak at 2856 cm^{-1} was obtained which corresponds to the symmetric stretching of the $–CH_2$ groups.[34] Due to the long alkyl chain of HDTMS, the intensity of the peak is significantly high, confirming the presence of HDTMS on the fabric surface.

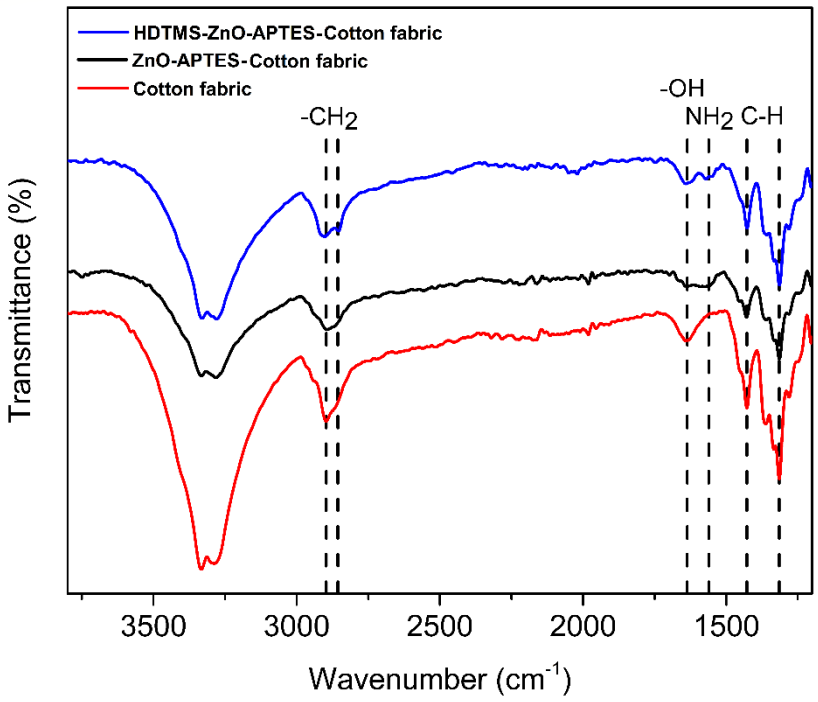

Figure 8. FTIR spectra of HDTMS-ZnO-APTES-Cotton fabric through the different stages of sample preparation

To identify the crystal structure of the ZnO nanoparticles deposited on the fabric surface, XRD analysis was conducted as shown in Figure 9. All the fabric samples through the different stages

of preparation contain the monoclinic crystal structure of cellulose I due to the cotton fabric which was confirmed by the presence of peaks at 14.97°, 16.49°, 22.73° and 34.57° corresponding to the (-110), (110), (200), and (004) planes respectively (ICDD #00-056-1718). After modifying the fabric with ZnO nanoparticles using APTES, characteristic peaks of ZnO hexagonal zincite structure were observed. This was confirmed by the presence of peaks at 32.01°, 34.63°, 36.43°, 47.69°, 56.77°, 63.09°, 68.15° and 69.25° which corresponds to the (100), (002), (101), (102), (110), (103), (112) and (201) planes respectively (ICDD #04-006-2557). No significant variation in peak position and peak intensity was observed after coating with HDTMS, which confirms that HDTMS does not interfere with the ZnO phase upon deposition.

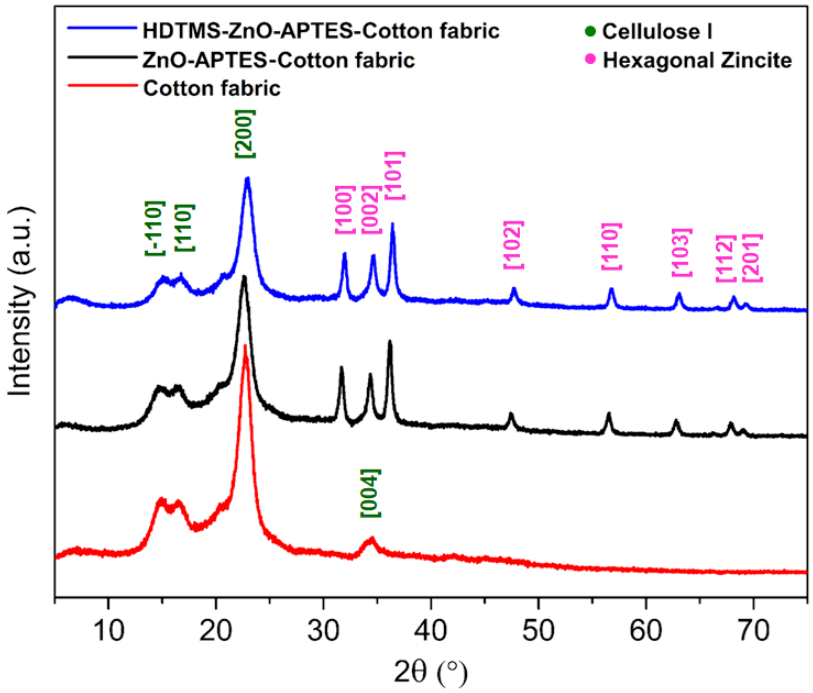

Figure 9. XRD patterns for phase identification of ZnO for HDTMS-ZnO-APTES-Cotton fabrics through various stages of sample preparation

3.4 UV blocking performance

Pristine cotton fabric lacks the ability to protect the wearer from the harmful UV rays of the sun. To be shielded from the UV radiation, the fabric should have an ultraviolet protection factor (UPF) rating of 50. The UV blocking ability of the as-prepared fabrics was evaluated by the AATCC 183-2004 Test Method.[29] The UPF rating, the percentage transmission in the UV-A and the UV-B region was recorded as shown in Table 2. The pristine cotton fabric displays a low UPF of 7.9, insufficient to block the UV rays completely to safeguard the wearer. The ZnO-treated fabrics, with and without HDTMS coating, both display very high UPF rating, over 200 times more than pristine cotton fabric. Additionally, the transmission of UV-A and UV-B rays through the ZnO-treated fabrics is lower than 0.5%, manifesting excellent UV blocking ability of the as-prepared fabrics (Figure 10). Therefore, by the incorporation of ZnO nanoparticles through this novel fabrication technique, the multi-functional fabric displays superhydrophobic, antibacterial and UV-blocking properties, making it desirable for clothing applications.

Table 2 The UV-blocking parameters of HDTMS-ZnO-APTES-Cotton fabrics through various stages of sample preparation

Sample Type	T (UVA) %	T (UVB) %	UPF
Pristine Cotton fabric	17.8 ± 0.2	10.2 ± 0.2	7.9 ± 0.1
ZnO-APTES-Cotton fabric	0.3 ± 0.04	0.05 ± 0.01	1650.3 ± 349.1
HDTMS-ZnO-APTES-Cotton fabric	0.2 ± 0.06	0.05 ± 0.01	1769.2 ± 304.3

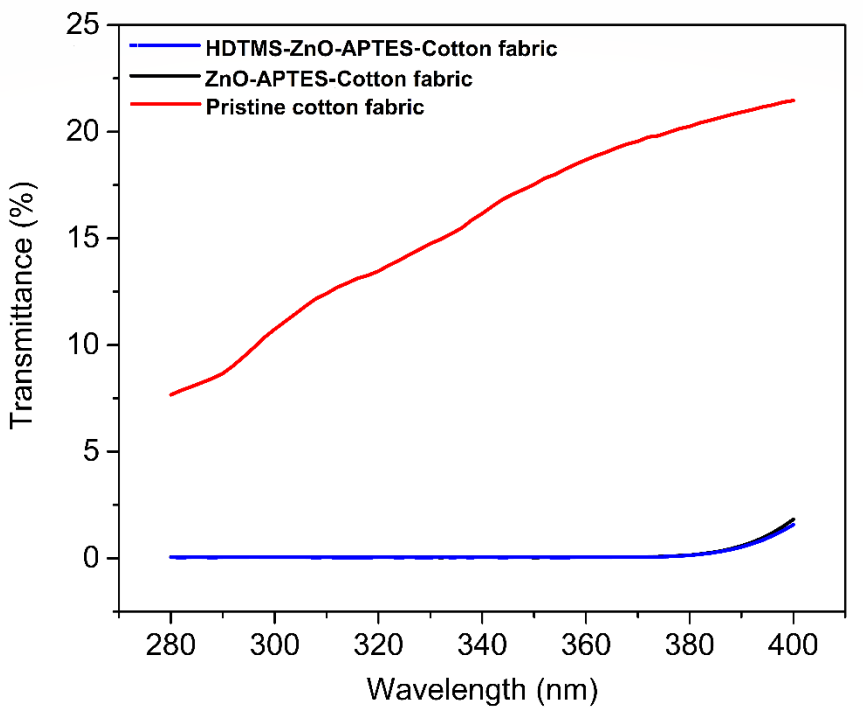

Figure 10. Transmittance of HDTMS-ZnO-APTES-Cotton fabrics within the UV region through different stages of sample preparation

3.5 Durability measurements

For the fabrics to be commercially viable, it is essential for them to display long-lasting durability. The as-prepared fabrics were subjected to 800 cycles of abrasion and the performance is shown in Figure 11. With an increase in the number of abrasion cycles, there was a gradual decrease in superhydrophobicity marked by a small decrease in WCA and an increase in WSA. Abrasion causes the wear of the fibres, damages the coating and affects the dual scale roughness essential for displaying superhydrophobicity. The HDTMS layer damage could have also been responsible in lowering of the WCA with increasing abrasion cycles. However, even after the 800 cycles of abrasion, the as-prepared fabrics displayed high durability. Based on the FE-SEM images, the ZnO nanoparticles were still adhered to the fabric surface after the abrasion test (Figure S4, Supporting

Information). This confirms the robustness of the synthesized coating through this dual silanization approach.

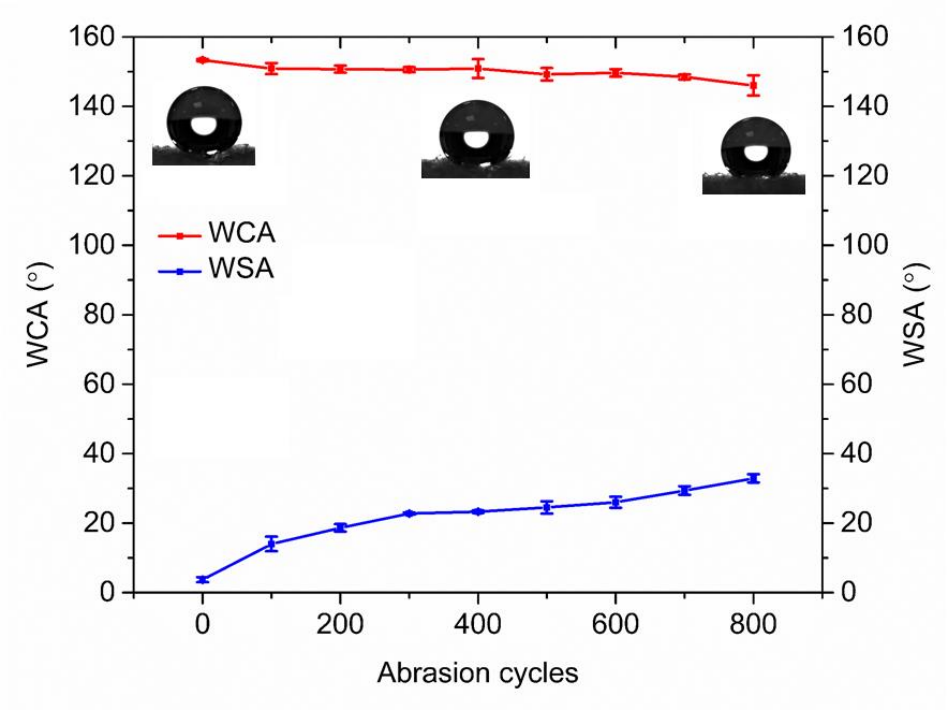

Figure 11 The effect of abrasion cycles on the WCA and WSA for HDTMS-ZnO-APTES-Cotton fabrics

The wash-fastness of the as-prepared fabrics was evaluated by subjecting them to ultrasonic washing for 2 hours in the solution of a non-ionic detergent, Triton-X. The effect of ultrasound on WCA and WSA at periodic intervals of 15 minutes is shown in Figure 12. Despite the high temperature and pressure regions created on the fabric surface due to the ultrasound waves, the fabrics displayed long lasting durability. There was only a small decrease in WCA from 151.9° to 148.9° and a moderate WSA increase from 2.4° to 14.9°. This test confirms the durability of the as-prepared fabrics to washing when used for clothing or healthcare applications.

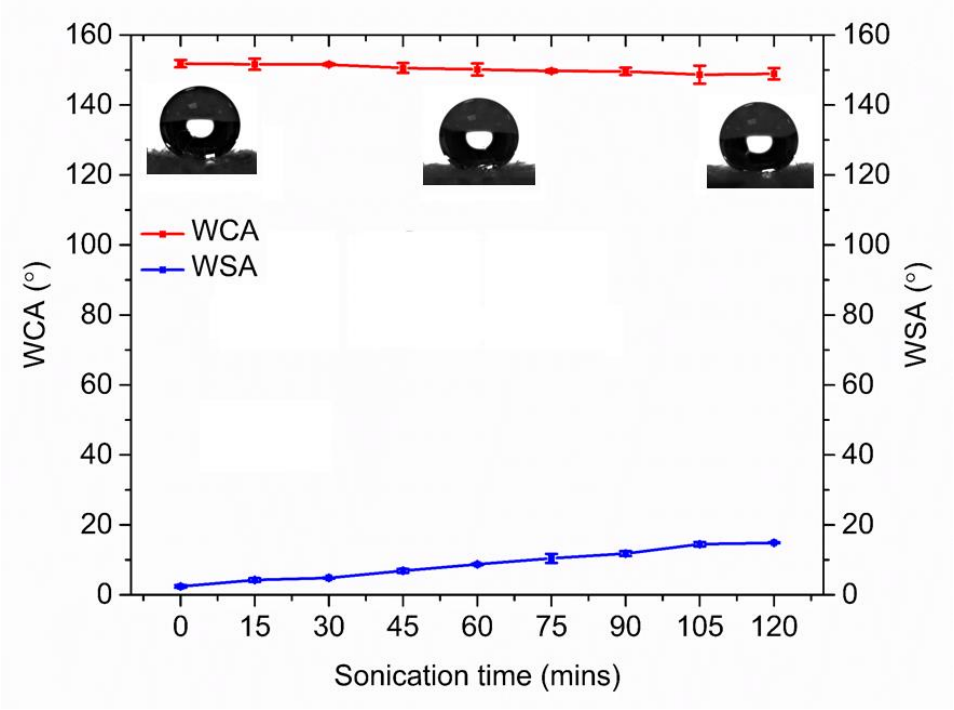

Figure 12. The effect of ultrasonic washing on the WCA and WSA for HDTMS-ZnO-APTES-Cotton fabrics

The chemical stability of the as-prepared fabrics was evaluated by submerging them in aqueous solutions of NaOH and HCl with pH ranging from pH = 1 to pH = 13 for a period of 24 hours and the effect on WCA and WSA is shown in Figure 13. The fabrics displayed high stability against the acidic and alkaline environments between pH = 3 to pH = 11. The WCA remained > 150° and the WSA < 15° showing high resistance to chemical changes. However, at extreme pH conditions of pH = 1 - 3, the performance of the coating was compromised. ZnO is an amphoteric oxide and therefore, reacts with both HCl and NaOH at extreme pH values resulting in the dissolution of the nanoparticles on the fabric surface. In such solutions, the WCA was reduced to 146° and the WSA rose to 25° and 32° for pH = 1 and pH = 13, respectively. However, such extreme conditions are rarely encountered in everyday situations and therefore, the fabrics display satisfactory durability under commonly occurring chemical solutions.

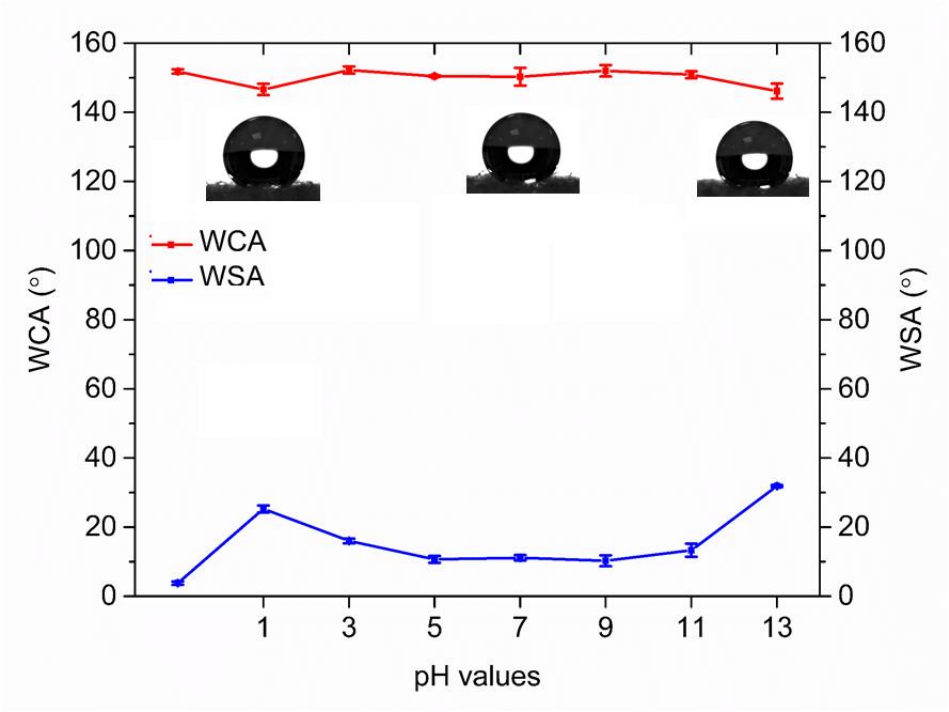

Figure 13. The effect of pH on the WCA and WSA for HDTMS-ZnO-APTES-Cotton fabrics

To evaluate the longevity of the UV-blocking ability of the as-prepared fabrics, they were subjected to UV irradiance for a period of 12 hours and the variation in WCA and WSA are displayed in Figure 14. Exposure to UV is known to cause degradation of a coating by causing chain scission reactions.[35] However, the ZnO nanoparticles incorporated on the fabric surface absorbed the UV rays, thereby protecting the coating from undergoing degradation. As a result, despite continuous UV exposure for 12 hours, there was no significant reduction in the superhydrophobicity of the fabrics. The WCA only dropped slightly from 152.9° to 149.2° while the WSA increased from 1.9° to 9.7° but still retaining the superhydrophobic performance. Hence, the fabrics displayed excellent durability against UV irradiation making the fabrics useful for UV-blocking applications.

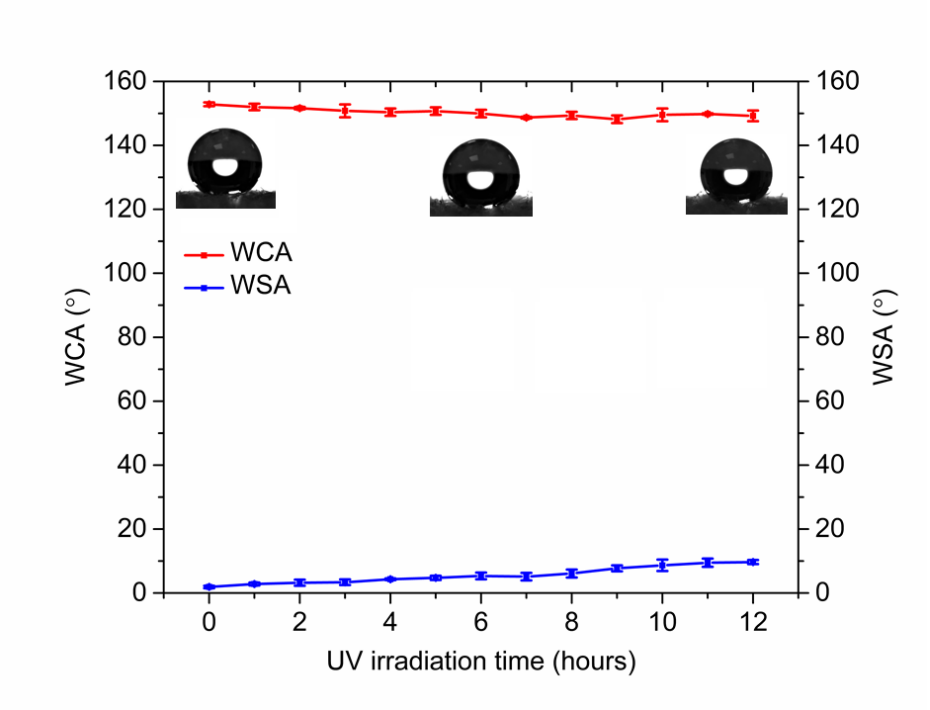

Figure 14 The effect of UV radiation on the WCA and WSA for HDTMS-ZnO-APTES-Cotton fabrics

Additionally, the thermal stability of the as-prepared fabrics was evaluated by thermogravimetric analysis (TGA). The result with discussion is given in Section S4 of the Supporting Information.

3.6 Air permeability and flexural rigidity

The air permeability and flexural rigidity of the as-prepared fabrics was evaluated before and after the coating. The results are summarized in Table 3. The pristine cotton fabric displayed an air permeability of 1895 mm/s. After deposition of ZnO nanoparticles, the air permeability reduced to 1645 mm/s. This was due to the blocking of the air space between the fibres obstructing the air flow. After coating with HDTMS, the air permeability decreased marginally from 1645 mm/s to

1591 mm/s. Overall, the reduction in air permeability was 16% compared to the pristine cotton, thereby not affecting the breathability or wearer comfort for clothing applications.

A trend similar to air permeability was observed for flexural rigidity of the as-prepared fabrics (Table 3). The pristine cotton fabric displayed a flexural rigidity of 36.5 mg × cm. Upon coating of ZnO nanoparticles, the flexural rigidity of the fabric increased by 17%. The rigidity was further increased by 15% after HDTMS coating. However, the overall flexural rigidity of HDTMS-ZnO-APTES-Cotton fabric was merely 50.7 mg × cm, insignificant to alter the fabric quality, hence proving its applicability for the textile industry.[36]

Table 3 Air permeability and flexural rigidity data for HDTMS-ZnO-APTES Cotton fabrics through the various stages of sample preparation

Sample Type	Air permeability (mm/s)	Flexural rigidity (mg × cm)
Pristine cotton fabric	1895 ± 21.9	36.5
ZnO-APTES-Cotton fabric	1644.8 ± 48.9	44.1
HDTMS-ZnO-APTES-Cotton fabric	1591.1 ± 26.0	50.7

3.7 Self-cleaning application

To evaluate the self-cleaning ability of the as-prepared fabrics, graphite powder, a model contaminant (< 20 μm in size), was sprinkled on the fabric surfaces as shown in Figure 15a. During the test, water was dropped on the fabric using a pipette to wash away the dirt and the outcome is displayed in Figure 15b. For the pristine cotton fabric, the dirt accumulated on its hydrophilic surface leaving it stained and wet. For the ZnO-APTES-Cotton fabric, a similar result was obtained. Although the water droplets initially formed beads on the fabric surface, they were quickly absorbed leaving the dirt in its place. This clearly indicates that despite the presence of

dual-scale roughness, the absence of low surface energy has prevented the ZnO-APTES-Cotton fabrics from displaying any self-cleaning behaviour. On the contrary, the superhydrophobic fabric, treated with HDTMS to lower the surface energy, successfully displayed self-cleaning ability. Most of the dirt rolled away with the water droplets leaving the fabric surface clean and dry. Few dirt particles stuck between the fibres were easily removed by gently shaking the fabric. These results manifest the potential of the as-prepared fabrics for clothing applications.

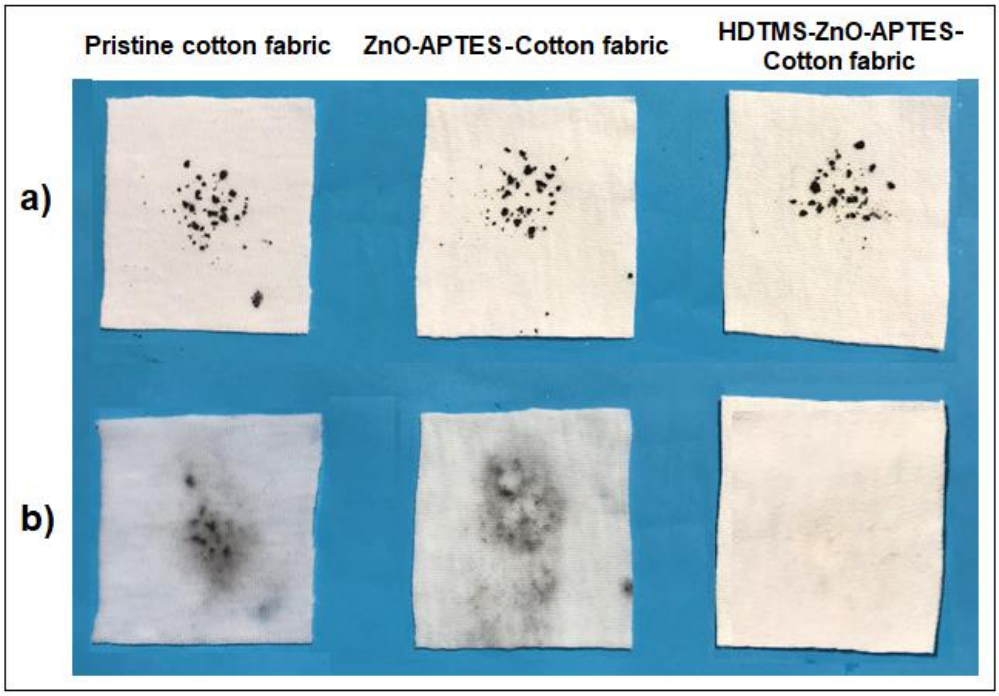

Figure 15 Evaluation of self-cleaning behaviour of HDTMS-ZnO-APTES-Cotton fabrics a) before the test b) after the test

4. Conclusion

In this work, successful fabrication of robust superhydrophobic antibacterial and ultraviolet-blocking cotton fabrics has been reported through a dual silanization approach. Zinc oxide nanoparticles were deposited on the surface of the pristine cotton fabric using APTES silane cross-linker and was further modified with HDTMS silane hydrophobe. The dual silanization resulted

in highly durable and multi-functional coatings on fabrics. They demonstrated superior resistance against abrasion, ultrasonic washing, chemical solution soaking and UV irradiation. The breathability and flexural rigidity of the fabrics were largely uncompromised after the coating. The fabrics retained their white appearance, thus making them suitable for clothing and healthcare applications. Overall, this technique is simple, cost-effective, eco-friendly and displays tremendous potential for various textile and surface engineering applications.

References

[1] W. Barthlott, C. Neinhuis, *Planta* **1997**, *202*, 1.

[2] S. Li, J. Huang, Z. Chen, G. Chen, Y. Lai, *J. Mater. Chem. A* **2017**, *5*, 31.

[3] a) Ç. Koşak Söz, S. Trosien, M. Biesalski, *ACS Appl. Mater. Interfaces* **2018**, *10*, 37478; b) N. Wang, D. Xiong, S. Pan, Y. Deng, Y. Shi, K. Wang, *Appl. Surf. Sci.* **2016**, *389*, 354.

[4] a) P. F. Rios, H. Dodiuk, S. Kenig, *Surf. Eng.* **2009**, *25*, 89; b) V. A. Ganesh, H. K. Raut, A. S. Nair, S. Ramakrishna, *J. Mater. Chem.* **2011**, *21*, 16304.

[5] a) G. Y. Bae, B. G. Min, Y. G. Jeong, S. C. Lee, J. H. Jang, G. H. Koo, *J. Colloid Interface Sci.* **2009**, *337*, 170; b) N. A. Ivanova, A. K. Zaretskaya, *Appl. Surf. Sci.* **2010**, *257*, 1800; c) Y. Shi, Y. Wang, X. Feng, G. Yue, W. Yang, *Appl. Surf. Sci.* **2012**, *258*, 8134; d) Y. Liu, J. H. Xin, C. H. Choi, *Langmuir* **2012**, *28*, 17426; e) L. Xu, R. G. Karunakaran, J. Guo, S. Yang, *ACS Appl. Mater. Interfaces* **2012**, *4*, 1118; f) M. Zhang, S. Wang, C. Wang, J. Li, *Appl. Surf. Sci.* **2012**, *261*, 561; g) J. Liang, Y. Zhou, G. Jiang, R. Wang, X. Wang, R. Hu, X. Xi, *J. Text. Inst.* **2013**, *104*, 305; h) E. Richard, R. V. Lakshmi, S. T. Aruna, B. J. Basu, *Appl. Surf. Sci.* **2013**, *277*, 302; i) M. Yu, Z. Wang, H. Liu, S. Xie, J. Wu, H. Jiang, J. Zhang, L. Li, J. Li, *ACS Appl. Mater. Interfaces* **2013**, *5*, 3697; j) J. Wang, G. Geng, A.

Wang, X. Liu, J. Du, Z. Zou, S. Zhang, F. Han, *Ind. Crops and Prod.* **2015**, *77*, 36; k) Q. Gao, J. Hu, R. Li, L. Pang, Z. Xing, L. Xu, M. Wang, X. Guo, G. Wu, *Carbohydr. Polym.* **2016**, *149*, 308.

[6] a) G. Meng, H. Peng, J. Wu, Y. Wang, H. Wang, Z. Liu, X. Guo, *Fibers Polym.* **2017**, *18*, 706; b) A. Berendjchi, R. Khajavi, M. E. Yazdanshenas, *Nanoscale Res. Lett.* **2011**, *6*, 594.

[7] a) C. Pan, L. Shen, S. Shang, Y. Xing, *Appl. Surf. Sci.* **2012**, *259*, 110; b) M. Shateri-Khalilabad, M. E. Yazdanshenas, *J. Text. Inst.* **2013**, *104*, 861.

[8] a) M. Shateri-Khalilabad, M. E. Yazdanshenas, *Cellulose* **2013**, *20*, 963; b) T. Suryaprabha, M. G. Sethuraman, *J. Alloys Compd.* **2017**, *724*, 240.

[9] a) M. Zhang, C. Wang, *Carbohydr. Polym.* **2013**, *96*, 396; b) T. Suryaprabha, M. G. Sethuraman, *Cellulose* **2018**, *25*, 3151.

[10] a) A. K. Singh, J. K. Singh, *New J. Chem.* **2017**, *41*, 4618; b) S. Afzal, W. A. Daoud, S. J. Langford, *J. Mater. Chem. A* **2014**, *2*, 18005.

[11] a) H. Wang, H. Zhou, A. Gestos, J. Fang, T. Lin, *ACS Appl. Mater. Interfaces* **2013**, *5*, 10221; b) H. Wang, H. Zhou, S. Liu, H. Shao, S. Fu, G. C. Rutledge, T. Lin, *RSC Adv.* **2017**, *7*, 33986.

[12] a) C. Jiang, W. Liu, M. Yang, C. Liu, S. He, Y. Xie, Z. Wang, *Appl. Surf. Sci.* **2019**, *463*, 34; b) S. Qiang, K. Chen, Y. Yin, C. Wang, *Mater. Des.* **2017**, *116*, 395.

[13] a) A. J. Patil, Y. Zhao, X. Liu, X. Wang, *Text. Res. J.* **2017**, *88*, 1788; b) J. Lin, X. Chen, C. Chen, J. Hu, C. Zhou, X. Cai, W. Wang, C. Zheng, P. Zhang, J. Cheng, Z. Guo, H. Liu, *ACS Appl. Mater. Interfaces* **2018**, *10*, 6124.

[14] a) L. Wang, X. Zhang, B. Li, P. Sun, J. Yang, H. Xu, Y. Liu, *ACS Appl. Mater. Interfaces* **2011**, *3*, 1277; b) G. Broasca, G. Borcia, N. Dumitrascu, N. Vrinceanu, *Appl. Surf. Sci.* **2013**, *279*, 272.

[15] a) M. Shateri Khalil-Abad, M. E. Yazdanshenas, *J. Colloid Interface Sci.* **2010**, *351*, 293; b) M. Shateri-Khalilabad, M. E. Yazdanshenas, A. Etemadifar, *Arabian J. Chem.* **2017**, *10*, S2355; c) S. Heinonen, E. Huttunen-Saarivirta, J.-P. Nikkanen, M. Raulio, O. Priha, J. Laakso, E. Storgårds, E. Levänen, *Colloids Surf., A* **2014**, *453*, 149.

[16] a) T. Suryaprabha, M. G. Sethuraman, *Cellulose* **2017**, *24*, 395; b) J. Yang, H. Xu, L. Zhang, Y. Zhong, X. Sui, Z. Mao, *Surf. Coat. Technol.* **2017**, *309*, 149.

[17] a) B. Xu, J. Ding, L. Feng, Y. Ding, F. Ge, Z. Cai, *Surf. Coat. Technol.* **2015**, *262*, 70; b) J. Y. Huang, S. H. Li, M. Z. Ge, L. N. Wang, T. L. Xing, G. Q. Chen, X. F. Liu, S. S. Al-Deyab, K. Q. Zhang, T. Chen, Y. K. Lai, *J. Mater. Chem. A* **2015**, *3*, 2825; c) L. Karimi, M. E. Yazdanshenas, R. Khajavi, A. Rashidi, M. Mirjalili, *Cellulose* **2014**, *21*, 3813.

[18] a) T. I. Shaheen, M. E. El-Naggar, A. M. Abdelgawad, A. Hebeish, *Int. J. Biol. Macromol.* **2016**, *83*, 426; b) N. Ghasemi, J. Seyfi, M. J. Asadollahzadeh, *Cellulose* **2018**, *25*, 4211; c) V. Pandiyarasan, S. Suhasini, J. Archana, M. Navaneethan, A. Majumdar, Y. Hayakawa, H. Ikeda, *Appl. Surf. Sci.* **2017**, *418*, 352.

[19] A. Sirelkhatim, S. Mahmud, A. Seeni, N. H. M. Kaus, L. C. Ann, S. K. M. Bakhori, H. Hasan, D. Mohamad, *Nano-Micro Lett.* **2015**, *7*, 219.

[20] K. S. Siddiqi, A. ur Rahman, Tajuddin, A. Husen, *Nanoscale Res. Lett.* **2018**, *13*, 141.

[21] P. M. Narayanan, S. Wilson, A. Thomas Abraham, M. Sevanan, *BioNanoScience*, **2012,** *2*, 329.

[22] R. Borda d' Água, R. Branquinho, M. P. Duarte, E. Maurício, A. L. Fernando, R. Martins, E. Fortunato, *New J. Chem.* **2018**, *42*, 1052.

[23] L. Xu, X. Zhang, Y. Shen, Y. Ding, L. Wang, Y. Sheng, *Ind. Eng. Chem. Res.* **2018**, *57*, 6714.

[24] M. Shateri-Khalilabad, M. E. Yazdanshenas, *Text. Res. J.* **2013**, *83*, 993.

[25] a) L. Windler, M. Height, B. Nowack, *Environ. Int.* **2013**, *53*, 62; b) R. Dastjerdi, M. Montazer, *Colloids Surf. B Biointerfaces* **2010**, *79*, 5.

[26] E. S. Ates, H. E. Unalan, *Thin Solid Films* **2012**, *520*, 4658.

[27] a) S. Pal, S. Mondal, J. Maity, *Mater. Technol.* **2018**, *33*, 555; b) V. Prasad, A. Arputharaj, A. K. Bharimalla, P. G. Patil, N. Vigneshwaran, *Appl. Surf. Sci.* **2016**, *390*, 936; c) N. Preda, M. Enculescu, I. Zgura, M. Socol, E. Matei, V. Vasilache, I. Enculescu, *Mater. Chem. Phys.* **2013,** *138*, 253.

[28] J. Zimmermann, S. Seeger, F. A. Reifler, *Text. Res. J.* **2009**, *79*, 1565.

[29] in *AATCC Technical Manual*, Vol. *85*, New York, N.Y: Published for the Association by Howes Pub. Co., 2010.

[30] in *AATCC Technical Manual*, Vol. *85*, New York, N.Y: Published for the Association by Howes Pub. Co., 2010.

[31] J. Kim, *Interfaces and Interphases in Analytical Chemistry*, Vol. *1062*, American Chemical Society **2011**, Ch. 6, pp. 141.

[32] P. Garside, P. Wyeth, *Stud. Conserv.* **2003**, *48*, 269.

[33] N. Majoul, S. Aouida, B. Bessaïs, *Appl. Surf. Sci.* **2015**, *331*, 388.

[34] a) L. Xu, L. Wang, Y. Shen, Y. Ding, Z. Cai, *Fibers Polym.* **2015**, *16*, 1082; b) H. Chang, K. Tu, X. Wang, J. Liu, *RSC Adv.* **2015**, *5*, 30647.

[35] K. Efimenko, W. E. Wallace, J. Genzer, *J. Colloid Interface Sci.* **2002**, *254*, 306.

[36] H. M. Elder, P. K. Guha-Thakurta, S. R. Ranganathan, *J. Text. Inst.* **1970**, *61*, 88.

Table of Contents

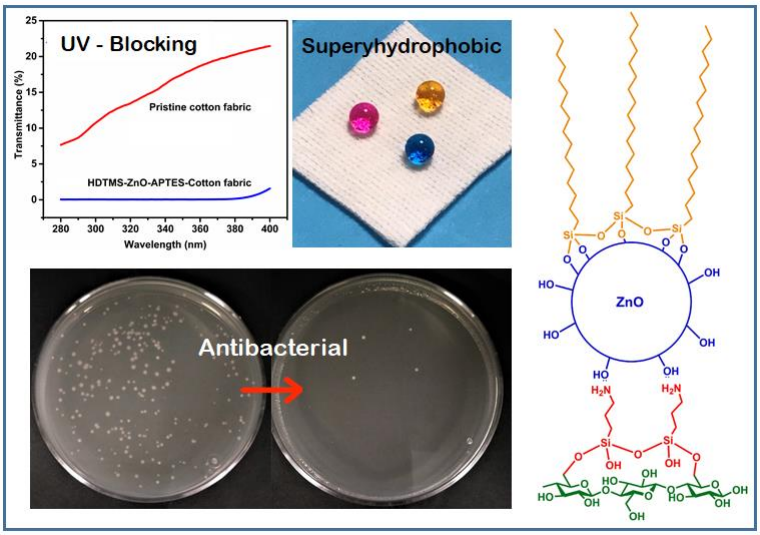

Multifunctional cotton fabrics have been prepared by a dual stage silanization approach where the zinc oxide nanoparticles are anchored to the cotton fabric by a silane cross-linker followed by modification with a silane hydrophobe. This facile procedure has resulted in highly functional superhydrophobic antibacterial and UV-blocking fabrics with excellent durability against abrasion, ultrasonic washing, immersion in different pH solutions, and prolonged UV irradiation.

Keywords: superhydrophobic antibacterial UV blocking fabrics